Molecular Therapy
Nucleic Acids
Original Article

Factor VII-Induced MicroRNA-135a Inhibits Autophagy and Is Associated with Poor Prognosis in Hepatocellular Carcinoma

Kuang-Tzu Huang,[1,2] I-Ying Kuo,[2] Ming-Chao Tsai,[3] Chun-Hsien Wu,[2] Li-Wen Hsu,[2] Li-Yu Chen,[2] Chao-Pin Kung,[1,2] Yu-Fan Cheng,[4] Shigeru Goto,[5] Yu-Wei Chou,[6] Chao-Long Chen,[1,2] Chih-Che Lin,[2,7] and Kuang-Den Chen[1,2,7]

[1]Institute for Translational Research in Biomedicine, Kaohsiung Chang Gung Memorial Hospital, Kaohsiung 83301, Taiwan; [2]Liver Transplantation Center, Department of Surgery, Kaohsiung Chang Gung Memorial Hospital, Kaohsiung 83301, Taiwan; [3]Division of Hepato-gastroenterology, Department of Internal Medicine, Kaohsiung Chang Gung Memorial Hospital, Kaohsiung 83301, Taiwan; [4]Department of Diagnostic Radiology, Kaohsiung Chang Gung Memorial Hospital, Kaohsiung 83301, Taiwan; [5]Fukuoka Institute of Occupational Health, Fukuoka 815-0081, Japan; [6]Tissue Bank and BioBank, Kaohsiung Chang Gung Memorial Hospital, Kaohsiung 83301, Taiwan

Hepatocellular carcinoma (HCC) is one of the most common and aggressive malignancies worldwide. Treatment outcomes remain poor mainly due to lack of good diagnostic/prognostic markers and limited therapeutic strategies. We previously characterized aberrant activation of the TF/FVII/PAR2 pathway, which subsequently results in decreased autophagy, as a crucial event in malignant progression of HCC.

Here, we identified miR-135a as a highly upregulated miRNA in HCC in response to TF/FVII/PAR2 activation. Analyzing 103 HCC patient specimens, we confirmed that miR-135a was frequently elevated in HCC tissues with higher FVII expression compared to adjacent non-cancerous counterparts. Increased miR-135a levels in HCC were also associated with tumor staging, recurrence, microvascular invasion, and decreased disease-free survival. We subsequently identified Atg14, a key component that regulates the formation of autophagosome as a direct target of miR-135a. Ectopic expression of miR-135a suppressed Atg14 levels and inhibited the autophagic processes. Our results indicate strong positive correlations between miR-135a levels and malignant behaviors in HCC patients and also suggest novel functions of miR-135a in regulation of autophagy, which could be useful as a potential target for prognostic and therapeutic uses.

INTRODUCTION

Hepatocellular carcinoma (HCC), the major subtype of primary liver cancers, is among the most common malignancies and third leading cause of cancer deaths worldwide.[1,2] Incidence of HCC is more than half a million cases each year.[3] Progression of chronic liver diseases to HCC may take decades; however, by the time the cancer is detected, prospects for successful treatment are less than desirable. Despite significant advances in therapeutic strategies including surgical resection, loco-regional ablation therapy, and liver transplantation, prognosis remains poor for high rate of tumor recurrence and metastasis following treatment.[4,5] Unfortunately, the underlying mechanisms of high recurrence rate are largely unclear. Therefore, there is an urgent need to understand the tumorigenic mechanisms of HCC and develop effective diagnostics and treatment options for this disease.

MicroRNAs (miRNAs) are small non-coding RNAs (usually 18–24 nucleotides in length) that regulate gene expression by directly targeting mRNA for degradation or suppressing protein translation by binding to the 3′ untranslated region (3′ UTR) of target mRNAs,[6,7] providing an intricate way to fine-tune gene expression. MiRNAs participate in a wide variety of biological processes and can act as oncogenes or tumor suppressors depending on cellular contexts in various human cancers.[8] Numerous studies indicate that aberrant expression of miRNAs can be used as potential diagnostic or prognostic tools for malignancies including HCC as tumor-derived miRNAs circulate in a relatively stable form.[9,10] For example, miR-122 and miR-199a/b-3p are among the highest liver-expressing miRNAs and consistently downregulated in HCC.[11,12] Moreover, miRNAs including miR-125b and miR-494 have been shown to regulate HCC growth and invasion[13,14] and may emerge as useful tools to control neoplastic behaviors.

Autophagy is a physiological process in which the cell sequesters part of its own constituents for lysosomal degradation and converts proteins and lipids into alternative life-preserving fuel through tough

Received 8 February 2017; accepted 3 October 2017;
https://doi.org/10.1016/j.omtn.2017.10.002.

[7]These authors contributed equally to this work.

Correspondence: Kuang-Den Chen, PhD, Institute for Translational Research in Biomedicine and Liver Transplantation Center, Department of Surgery, Kaohsiung Chang Gung Memorial Hospital, 123 Da-Pi Rd, Niao-Sung Dist, Kaohsiung 83301, Taiwan.
E-mail: dennis8857@gmail.com
Correspondence: Chih-Che Lin, MD, PhD, Liver Transplantation Center, Department of Surgery, Kaohsiung Chang Gung Memorial Hospital, 123 Da-Pi Rd, Niao-Sung Dist, Kaohsiung 83301, Taiwan.
E-mail: immunologylin@gmail.com

Table 1. The Top Five Upregulated and Downregulated miRNAs in HCC Tumor with Higher FVII Levels Than the Adjacent Normal Region

Symbol	Mature Sequence	miRBase ID	Fold Change (TH/TL[a])	Adjusted p Value
Top 5 Upregulated				
MIR135A1	hsa-miR-135a-5p	MI0000452	8.144	0.013
MIR30A	hsa-miR-30a-5p	MI0000088	6.104	0.005
MIR10B	hsa-miR-10b-5p	MI0000267	4.568	8.88E-16
MIR423	hsa-miR-423-5p	MI0001445	3.175	0.044
MIR486	hsa-miR-486-5p	MI0002470	2.825	1.04E-13
Top 5 Downregulated				
MIRLET7I	hsa-let-7i-5p	MI0000434	0.132	0.019
MIRLET7D	hsa-let-7d-5p	MI0000065	0.181	2.85E-04
MIR199B	hsa-miR-199b-3p	MI0000282	0.195	1.30E-07
MIR199A	hsa-miR-199a-3p	MI0000281	0.196	1.30E-07
MIR28	hsa-miR-28-3p	MI0000086	0.325	0.001

[a]TH, higher expression in tumor compared to adjacent non-tumor tissue area; TL, lower expression in tumor compared to adjacent tissue area.

times such as cellular stress and energy deprivation.[15] Upon initiation of autophagy, multiple signaling pathways converge on the autophagy-related (Atg) proteins, resulting in the formation of a double-membraned structure named the autophagosome. Recruitment of the Atg12-Atg5 complex and microtubule-associated protein 1 light chain 3 (LC3) is essential for this process and is widely used as a marker to monitor autophagy. These autophagosomes then fuse with lysosomes to form autolysosomes that lead to organelle breakdown and recycling of resulting catabolites.

Dysregulated autophagic pathways have been linked to various diseases, including cancer.[16] Despite a general acceptance that autophagy is a protective mechanism toward cell survival, recent studies have revealed an active role of autophagy in cell death.[17,18] For example, autophagy has been shown to be decreased in HCC.[19,20] Decreased autophagy levels are well correlated with tumor aggressiveness and poor prognosis of HCC.[19] We have previously demonstrated that the coagulation pathway actively participates in the autophagic process. Tissue factor (TF) and factor VII (FVII) negatively regulate autophagy through signaling of the protease-activated receptor PAR2, responsible for malignant progression and decreased disease-free survival in HCC.[21–23]

In an effort to search for potential mediators or effectors that link the TF/FVII/PAR2 pathway to the autophagic process, we performed mRNA and miRNA sequencing to comprehensively characterize differentially expressed patterns in HCC cases that had high levels of FVII. We discovered that miR-135a, a resultant of TF/FVII/PAR2 signaling, was frequently upregulated in HCC. We further demonstrated that the level of Atg14, a putative target of miR-135a and a regulatory subunit in the phosphatidylinositol 3-kinase (PI3K) complex, crucial in formation of autophagosome, negatively correlates with miR-135a expression both in vitro and in HCC cases. More importantly, elevated miR-135a inhibited the autophagic pathway and was associated with tumor progression, recurrence, and decreased disease-free survival of HCC. Overall, our data highlight a novel function of miR-135a in regulation of autophagy and suggest potential prognostic value of HCC.

RESULTS

Upregulation of miR-135a Is Observed in HCC Tumors with High FVII Expression

We have previously established an inverse correlation between the levels of FVII/TF/PAR2 proteins and autophagic factors in HCC. To search for potential effectors that are associated with this process, we performed mRNA and miRNA sequencing to comprehensively compare the expression profiles between cases of HCC with higher FVII levels in the tumor region and the contiguous histologically normal counterpart (n = 3). As shown in Table 1, the top five upregulated (fold change, 2.8 to 8.1) and top five downregulated (fold change, 0.33 to 0.13) miRNAs were listed. Among the miRNAs with altered expression, we specifically picked miR-135a to study for its strong implications in cancer progression. We first analyzed whether an aberrant increase in miR-135a expression occurred in HCC. The level of miR-135a was compared between HCC tumor and its adjacent normal region (patient demographic information in Table 2) using qRT-PCR. Interestingly, we found that in more than 85% of the cases (90 out of 103), miR-135a was upregulated in the tumor, strongly suggesting potential involvement in cancer development (Figure 1A).

To validate that the change in miR-135a expression was indeed an outcome of FVII/TF/PAR2 signaling, recombinant FVIIa, TF, or a PAR2 peptide agonist was administered to an HCC cell line, Hep3B, to determine miR-135a levels using qRT-PCR. As shown in Figure 1B, miR-135a levels were increased in response to all three types of treatments. Conversely, transfection of Hep3B cells with FVII, TF, or PAR2 small interfering RNA (siRNA) resulted in a decrease in miR-135a levels (Figure 1C). Our previous work established a role for TF/FVII/PAR2 signaling in inhibition of autophagy and promotion of HCC tumor progression through activation of extracellular signal regulated kinase 1/2 (ERK1/2) and subsequently tuberous sclerosis 2 (TSC2)/mammalian target of rapamycin (mTOR).[21–23] We further showed that miR-135a expression was also dependent upon mTOR levels, as we observed decreased miR-135a in mTOR knocked-down Hep3B cells (Figure 1D). To corroborate the above correlations in a clinical setting, we compared FVII protein levels with miR-135a expression in HCC tissues. Our data showed that in a combined 73% of all cases, patients with higher FVII in the tumor than the normal region (T > N) also had increased miR-135a expression; patients with lower FVII in the tumor (T < N) had decreased levels of miR-135a (Figure 1E, left). Quantitatively, patients with increased FVII protein levels in the tumor compared to the normal region (T > N) had a higher miR-135a tumor/normal ratio than those with decreased FVII (T < N) (Figure 1E, right).

Table 2. Demographic Information of the 103 HCC Patients in This Study

Age (years) (median; range)	59 (31–85)
Sex (M:F)	82:21
AFP (ng/mL) (median; range)	13.6 (1.63–500000)
Tumor size (cm) (median; range)[a]	5 (1.2–18.8)
Liver cirrhosis (+) (%)	61 (61)
Hepatitis (B, C, B + C, NBNC)	71, 14, 3, 15
TNM stage (I, II, III, IV)	28, 41, 16, 18

[a]Measured by the length of the largest tumor nodule.

Atg14, Component of the Autophagic Pathway, Is a Direct Target of miR-135a

Given the strong positive correlations between FVII and miR-135a in HCC, we next sought whether there was a potential link with autophagic factors. A miRDB search revealed that Atg14, a key subunit in the PI3K complex that regulates formation of autophagosomes, is a putative target of miR-135a. Figure 2A depicts the predicted target sequence of miR-135a in the 3′ UTR of the *atg14* gene. In Hep3B cells transfected with FVII siRNA, Atg14 expression was increased (Figure 2B). To examine whether miR-135a negatively regulated Atg14 levels, HCC cell lines Hep3B and HepG2 were transfected with a miR-135a mimic, and Atg14 mRNA levels were determined using qRT-PCR. Our results showed that overexpression of miR-135a resulted in a decrease in Atg14 expression (up to ~75% decrease in Hep3B, ~40% in HepG2) (Figure 2C). To show whether miR-135a directly targeted the 3′ UTR of *atg14* gene, we established a reporter construct that contained the putative miR-135a target sequence downstream of the firefly luciferase gene. Transfection of the reporter construct together with miR-135a mimic into Hep3B cells resulted in ~45% decrease in luciferase activity, whereas no significant difference was observed in cells transfected with the construct containing a mutated binding site (Figure 2D). These results suggest that Atg14 is a direct target of miR-135a activity and implicate that miR-135a may be involved in autophagy.

Correlations between miR-135a, Atg14, and Clinicopathological Characteristics in HCC Patients

With the observation that miR-135a targeted Atg14 for post-transcriptional repression, we next sought whether there was an association between levels of these two factors in clinical cases. We compared the ratios of Atg14 and miR-135a expression in HCC and the adjacent non-tumor tissues and found a significant inverse correlation ($R = -0.22$, $p = 0.024$) (Figure 2E), corroborating with our in vitro findings.

We further performed an association analysis between miR-135a expression and clinicopathological parameters in these HCC cases, categorized into miR-135a T > N (tumor > normal) and miR-135a T < N (tumor < normal) groups. The results indicated that in addition to Atg14 mRNA expression, hepatitis virus status, hepatitis B surface antigen (HBs-Ag), primary tumor stage, microvascular invasion, and alpha-fetoprotein (AFP) levels (cut-off = 70 ng/mL)[24] were significantly associated with miR-135a expression (Table 3), suggesting an involvement in HCC development and progression. Importantly, these cases were followed up for tumor recurrence and survival. Tumor recurrence was associated with miR-135a levels (Table 3). Moreover, patients with higher miR-135a in the tumor (T > N) had significantly shorter disease-free survival ($p = 0.009$) than those with lower expression in the tumor (T < N) (Figure 2F).

Combining Relative miR-135a Expression with AFP Levels Better Predicts Tumor Recurrence Than Assessing Using AFP Alone

AFP has been commonly considered the ideal serological marker for detecting tumors and proposed as a clinical predictor of tumor recurrence after surgery and other supplementary treatments for HCC. However, the poor sensitivity of AFP for HCC recurrence limits its clinical use. In the 103 HCC clinical cases, the sensitivity and specificity of AFP tests (cut-off = 70 ng/mL) were 44.4% and 75%, respectively. The weak sensitivity in predicting HCC recurrence resulted from cases in which reviving tumors were observed in more than 50% (35/65 = 53.8%) with preoperative AFP < 70 ng/mL. However, higher miR-135a levels in tumors compared to the adjacent areas (T > N) represented much higher sensitivity (95.2%) but lower specificity (25%) in predicting recurrent events. Prognostic assessment by applying miR-135a together with serum AFP levels was therefore evaluated as illustrated in Figure 3. We found that in cases with AFP levels $\geq$ 70 ng/mL, recurrent and non-recurrent rates were very similar by assessing preoperative AFP alone or in combination with miR-135a expression (10 versus 9 non-recurrent cases; Figure 3, left red box). However, in cases with AFP < 70 ng/mL, the false negative recurrent events by combining AFP and miR-135a was only 3 out of 65 cases (AFP < 70 and miR-135a T < N) (Figure 3, middle red box), compared with those using preoperative AFP levels only (35 out of 65 cases with AFP < 70). The false positive rates by using AFP only (AFP $\geq$ 70; non-recurrent, 10/38) and AFP in combination with miR-135a (AFP < 70, miR-135a T > N; non-recurrent, 21/65; Figure 3, right red box) were comparable. The improvement in prognostic evaluation using the combinatorial assessment (sensitivity, 90.3%; specificity, 50%) also implies that miR-135a-mediated biological effects including autophagy suppression are key events responsible for HCC progression and poor survival, and thus the underlying mechanisms need further investigation.

miR-135a Inhibits Autophagic Processes In Vitro

So far, we have shown a strong correlation among FVII, miR-135a, and Atg14 levels in both in vitro and clinical cases. We therefore investigated whether miR-135a-induced downregulation of Atg14 affected the autophagic pathway. Hep3B or HepG2 cells were transfected with a miR-135a mimic, and autophagic markers were examined after 24 and 48 hr using immunoblotting. As shown in Figure 4A, overexpression of miR-135a resulted in an apparent decrease in Atg14 protein. LC3A/B, a protein marker of autophagosomes whose levels were well correlated with the number of autophagic vesicles, was also decreased. Other Atg proteins were examined in parallel. The

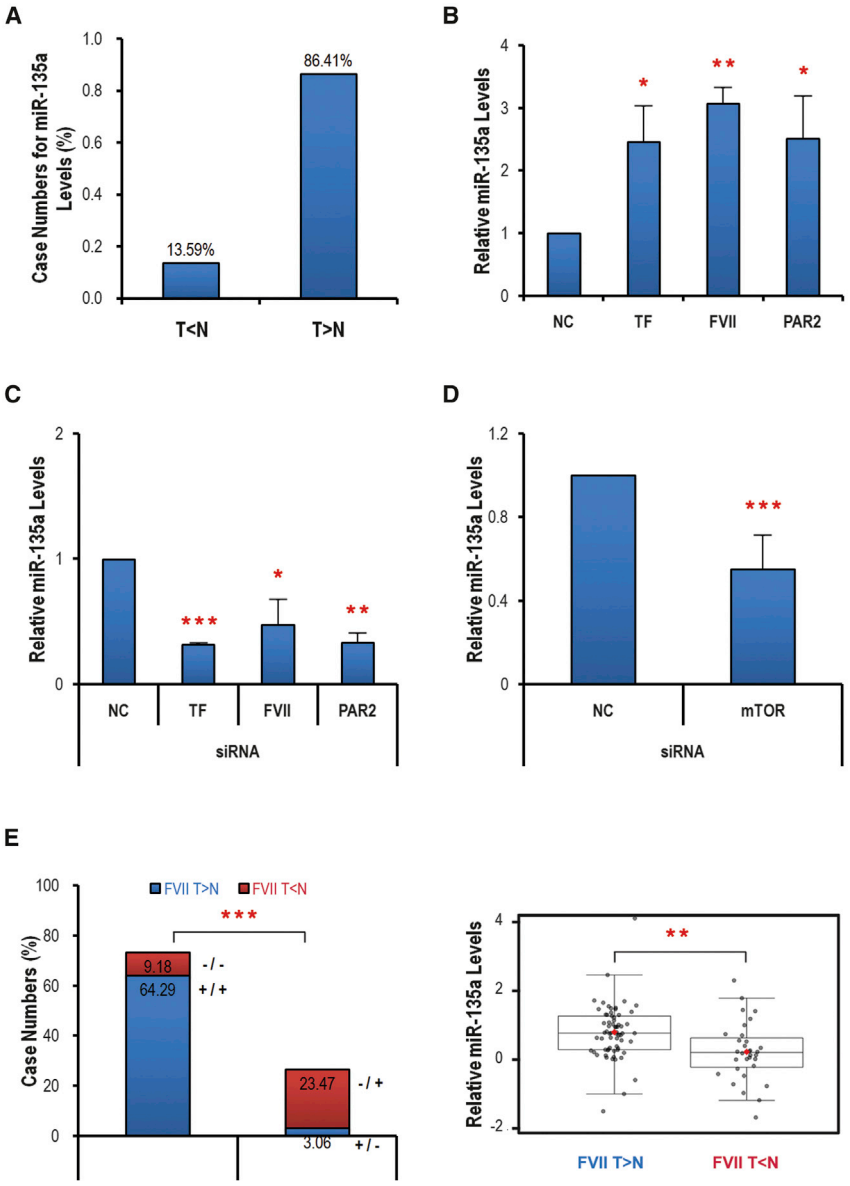

Figure 1. miR-135a Is Upregulated in HCC Tumor with High FVII Expression

(A) Expression of miR-135a was compared between HCC tumors (T) and their contiguous normal regions (N). (B) HCC cell line Hep3B was treated with recombinant TF, FVIIa, or a PAR2 peptide agonist for 24 hr. The level of miR-135a was analyzed. (C) Hep3B cells were transfected with siRNAs for TF, FVII, or PAR2. Expression of miR-135a was examined after 24 hr. (D) Hep3B cells were transfected with mTOR siRNA. The level of miR-135a was evaluated after 24 hr. (E) (Left) Correlations between FVII and miR-135a levels in HCC and non-tumor counterparts were assessed. We grouped patients having higher FVII and miR-135a levels in the tumor than the normal region (+/+) with patients having lower FVII and decreased miR-135a (−/−). These cases were compared with those having negatively correlated levels of FVII and miR-135a (+/− and −/+). (Right) Tumor/normal ratio of miR-135a expression was compared using qRT-PCR in HCC tumors that had higher FVII levels than the adjacent normal region (FVII T > N) and those that had lower FVII than the normal region (FVII T < N). The data are presented as mean ± SD. Statistically significant compared with controls at *$p < 0.05$; **$p < 0.01$; ***$p < 0.001$.

protein levels of Atg5, Atg7, and Atg12 were generally less affected upon miR-135a treatments (Figure 4B). As autophagy is a degradation mechanism involving lysosomes, protein expression of lysosomal marker LAMP-1 was assessed using immunoblotting. Transfection of miR-135a lowered the levels of LAMP-1 protein, suggesting a decrease in lysosome number (Figure 4C). A major lysosomal aspartic hydrolase, cathepsin D, was also examined. Targeted to the lysosomal vesicular structures, the 52-kDa pro-cathepsin D is cleaved at the N terminus to produce a single-chain intermediate enzyme called pre-cathepsin D. Further proteolytic cleavage yields the mature active proteases which comprise non-covalently linked heavy (34 kDa) and light (14 kDa) chains. Using an antibody that detects both the precursors and mature heavy chain of cathepsin D, we showed that the mature 34-kDa form was decreased, whereas the pro- and pre-cathepsin D forms were increased (Figure 4C). These results suggest that miR-135a has an inhibitory effect on autophagic processes, most likely due to downregulation of Atg14 and decreased lysosomal activity.

DISCUSSION

There have been a number of studies that demonstrate abnormalities in miRNA expression in HCC.[25–27] Nonetheless, miRNAs that modulate autophagy and their involvement in HCC progression have not been much addressed. In the current study, we discovered for the first time that miR-135a, upregulated in HCC with high FVII expression, inhibits autophagy by downregulating Atg14, a key element involved in the formation of autophagosomes. Elevated levels of miR-135a in HCC also represent tumor progression and decreased disease-free survival after curative resection, which implicates prognostic significance in patient management.

PAR2 is a member of a G protein-coupled receptor family that comprises surface proteins activated upon cleavage by specific serine proteases at the N-terminal domain. Activation of PAR2 has been linked to progression of various cancers.[28–30] Unlike other PAR family members, PAR2 is not activated by thrombin but can be cleaved by proteases including trypsin, chitinase, and activated FVIIa and FXa.[31] Notably, TF aberrantly expressed by tumor cells forms a functional complex with FVIIa and triggers multiple signaling pathways directed by PAR2. For example, TF/FVII/PAR2 initiates intracellular signals that activate protein kinase Cα and mitogen-activated protein

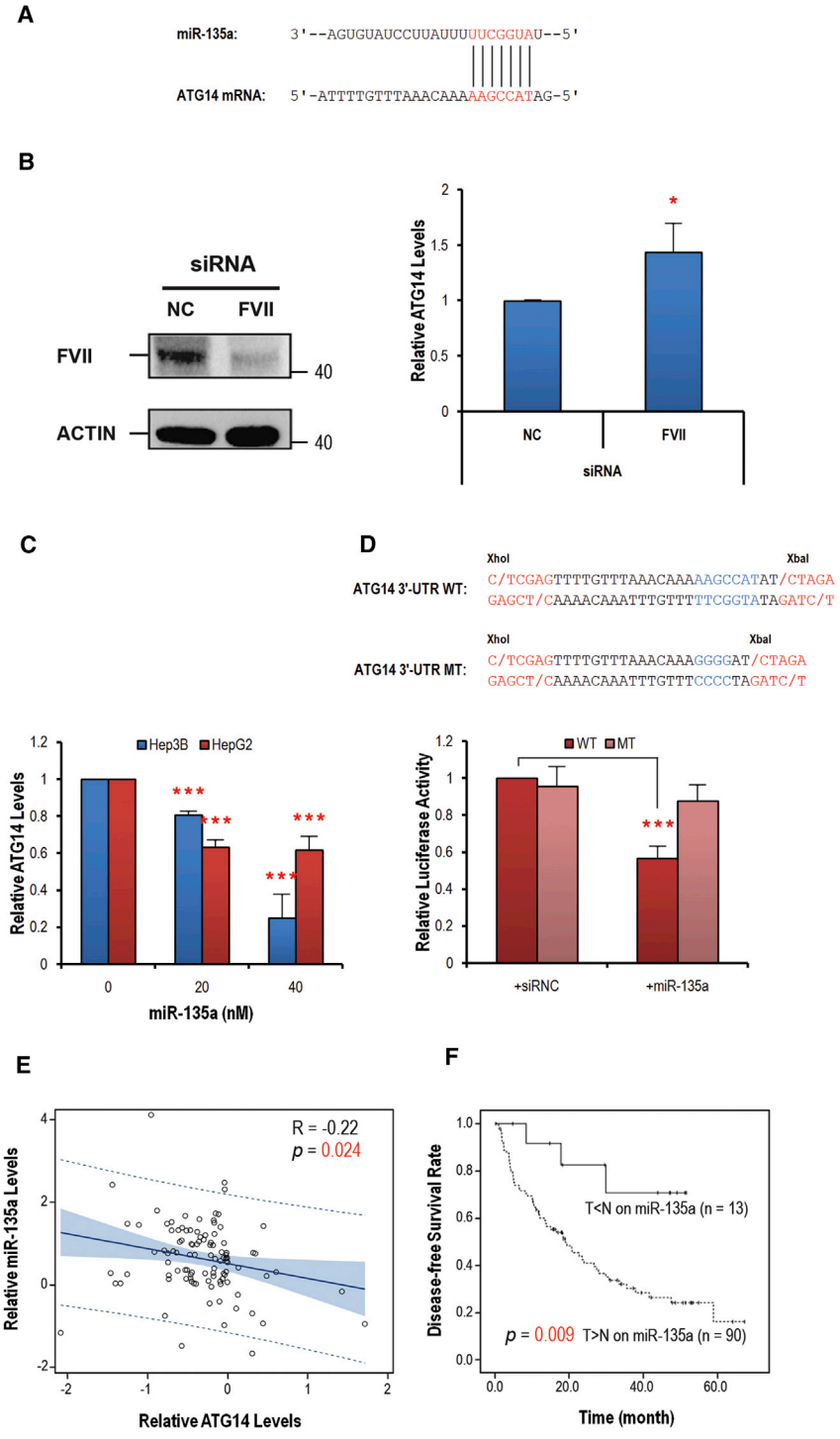

Figure 2. Atg14 Is a Direct Target of miR-135a

(A) Schematic representation of predicted miR-135a binding sequence at the 3′ UTR of *atg14* gene. (B) Hep3B cells were transfected with FVII siRNA for 24 hr. FVII protein (left) and Atg14 mRNA (right) levels were determined. (C) HCC cell lines Hep3B (left) and HepG2 (right) were transfected with a miR-135a mimic (20 nM, 40 nM), and the mRNA level of Atg14 was evaluated after 24 hr. (D) Hep3B cells were co-transfected with a miR-135a mimic and a reporter construct that contained the wild-type (WT) or mutated (MT) miR-135a binding sequence. Post-transcriptional repression was determined by measuring the relative luciferase activity. (E) Correlations of HCC tumor/normal ratios of Atg14 and miR-135a expression were depicted. (F) Kaplan-Meier probability distributions showing disease-free survival according to miR-135a levels in HCC tumors compared with their paired non-tumor tissues. The data are presented as mean ± SD. Statistically significant compared with controls at *$p < 0.05$; ***$p < 0.001$.

kinase (MAPK) p38, resulting in production of pro-angiogenic factors such as CTGF, VEGF, and interleukin-8 (IL-8), immune modulators such as macrophage colony-stimulating factor (M-CSF) and granulocyte-macrophage colony-stimulating factor (GM-CSF).[32–34] We previously showed that activation of TF/FVII/PAR2 signaling promotes HCC progression by inhibition of autophagy through TSC2/mTOR.[21,22] In this study, we further demonstrated that miR-135a expression is dependent upon mTOR levels and identified miR-135a as a downstream effector of PAR2 activation, which mediates post-transcriptional repression of its target gene Atg14 for abrogating the autophagic process.

Notably, miR-135a upregulation in HCC tumors occurs in more than 85% of our clinical cases. Our data also suggest a strong positive association between miR-135a and properties that indicate HCC progression, including tumor staging, microvascular invasion, and recurrence. Early detection of HCC recurrence after curative surgery is crucial for favorable prognosis. Clinically, conventional serum tumor markers together with imaging modalities are the most frequently used for recurrence assessment, while tremendous efforts are also being made to search for more reliable molecular targets. These serum markers, such as AFP and des-gamma-carboxy prothrombin (DCP; also known as PIVKA-II), can be problematic due to insufficient sensitivity and specificity issues that eventually limit the effectiveness. Indeed, in our current study of 103 HCC cases, we found using AFP levels (cut-off = 70 ng/mL) alone had low sensitivity in predicting HCC recurrence, while incorporating relative miR-135a expression improved the sensitivity. The limitation of this assessment is that only relative expression of miR-135a between tumor and normal regions is used, which makes it less applicable to pathological tests. However, using extracellular miRNA from body fluids such as

Table 3. Demographic and Clinicopathological Parameters of HCC Patients with miR-135a Levels Higher or Lower in Tumor Than the Adjacent Normal Region

Variable	Total	miR-135a T > N n (%)	miR-135a T < N n (%)	p Value
Atg14 mRNA Expression (T/N)				
T > N	13	6 (46.2)	7 (53.8)	p < 0.001
T < N	90	84 (93.3)	6 (6.7)	p < 0.001
Age				
≥50 years	85	74 (87.1)	11 (12.9)	p = 0.832
<50 years	18	16 (88.9)	2 (11.1)	p = 0.832
Sex				
Male	82	72 (87.8)	10 (12.2)	p = 0.797
Female	21	18 (85.7)	3 (14.3)	p = 0.797
Cirrhosis				
Present	61	52 (85.2)	9 (14.8)	p = 0.432
Absent	42	38 (90.5)	4 (9.5)	p = 0.432
Hepatitis				
B	71	68 (95.8)	3 (4.2)	p = 0.002
C	14	9 (64.3)	5 (35.7)	p = 0.002
B + C	3	2 (66.7)	1 (33.3)	p = 0.002
NBNC	15	11 (73.3)	4 (26.7)	p = 0.002
HBs-Ag				
Positive	74	70 (94.6)	4 (5.4)	p < 0.001
Negative	29	20 (69)	9 (31)	p < 0.001
Pathology Stage				
I, II	69	57 (82.6)	12 (17.4)	p = 0.038
III, IV	34	33 (97.1)	1 (2.9)	p = 0.038
T_stage				
1, 2	68	56 (82.4)	12 (17.6)	p = 0.032
3, 4	35	34 (97.1)	1 (2.9)	p = 0.032
N_stage				
n0	101	88 (87.1)	13 (12.9)	p = 0.587
n1	2	2 (100)	0 (0)	p = 0.587
M_stage				
n0	99	86 (86.9)	13 (13.1)	p = 0.438
n1	4	4 (100)	0 (0)	p = 0.438
Tumor Size				
≥5 cm	51	44 (86.3)	7 (13.7)	p = 0.738
<5 cm	52	46 (88.5)	6 (11.5)	p = 0.738
Tumor Number				
1	92	80 (87)	12 (13)	p = 0.505
2	7	7 (100)	0 (0)	p = 0.505
3	3	2 (66.7)	1 (33.3)	p = 0.505
4	1	1 (100)	0 (0)	p = 0.505
Recurrent				
Present	63	60 (95.2)	3 (4.8)	p = 0.003
Absent	40	30 (75)	10 (25)	p = 0.003
Microvascular Invasion				
Present	66	62 (93.9)	4 (6.1)	p = 0.007
Absent	37	28 (75.7)	9 (24.3)	p = 0.007
AFP				
<70 ng/mL	65	53 (81.5)	12 (18.5)	p = 0.02
≥70 ng/mL	38	37 (97.4)	1 (2.6)	p = 0.02
		mean (95% CI)	mean (95% CI)	
AST(U/L)	103	51.1 (40.9–61.2)	48.3 (28.6–68)	p = 0.845
ALT(U/L)	103	52.2 (42.3–61.9)	59.4 (23–95.9)	p = 0.612

T/N, tumor versus non-tumor adjacent tissue expression levels; HBs-Ag, hepatitis B virus surface antigen.

serum samples as biomarkers is promising but requires standardized procedures in collection, handling, and extraction methodologies. Quantification and calibration also affect data interpretation. Our present study still unravels an important area of research in which miR-135a may play a central role in HCC progression including autophagy suppression that ultimately leads to poor survival. We are now investigating whether circulating or exosomal miR-135a readily detectable in serum samples can be applied to our recurrence model.

Aberrant increase in miR-135a levels has also been observed in several other cancers, including breast, cervical, and colorectal cancers and melanoma.[35–38] The miR-135a targeted genes that contribute to malignant progression have been reported. For example, miR-135a is implicated in promotion of Wnt signaling by downregulating adenomatous polyposis coli (APC), tumor suppressor and key component of the Wnt pathway, and can induce nuclear β-catenin transactivation in the absence of the Wnt ligand.[37] Seven in absentia homolog 1 (SIAH1), an E3 ubiquitin ligase that directs β-catenin for proteasomal degradation,[39] has also been shown to be a target of miR-135a action.[36] Another miR-135a target gene and transcription factor, homeobox A10 (HOXA10), is associated with breast and ovarian cancers and endometriosis.[40] In liver cancer, miR-135a has been shown to repress metastasis suppressor 1 (MTSS1), a tumor suppressor that may be connected to portal vein tumor thrombus.[41] In the current study, the tumorigenic activity of miR-135a was mediated by direct repression of Atg14. Taken together, miR-135a post-transcriptionally regulates a network of genes that work collaboratively or independently on promotion of proliferative and invasive properties and may contribute, at least in part, to malignant progression of HCC and several other cancers.

Autophagy was initially considered a critical process that suppressed malignant transformation with a dynamic role of an early suppressor of tumor progression and a later event for pro-tumorigenic process.[20]

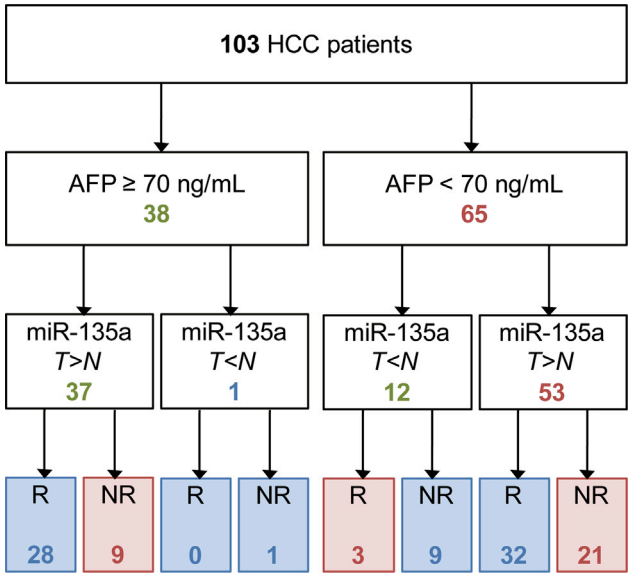

Figure 3. Combining Relative miR-135a Expression with AFP Levels Better Predicts Tumor Recurrence Than Assessing Using AFP Alone

Of the 103 HCC cases, patients were divided according to their preoperative AFP levels (cut-off = 70 ng/mL). Each group was then subcategorized based on the relative miR-135a expression in tumors compared to the adjacent normal areas (T > N or T < N). The number at the bottom of each box indicates case counts. R, recurrence; NR, non-recurrence.

In this study, we report miR-135a as a new autophagy-regulating miRNA by targeting Atg14. The levels of miR-135a and Atg14 were inversely correlated in our clinical cases. Ectopic expression of miR-135a resulted in inhibition of the autophagic process, as we observed decreased protein levels of autophagosome marker LC3A/B, lysosomal marker LAMP-1, and mature form of cathepsin D. Atg14 is a specific subunit in the PI3K complex, targeting the complex for proper autophagosome formation. PI3K complex activity is essential in the initiation process of autophagy in which phosphatidylinositol (PI) is phosphorylated by PI3K, allowing recruitment of downstream molecules required in autophagosome formation.[42] Atg14 acts as a connector and directs the PI3K complex efficiently to the phagophore assembly site.[43] In addition, Atg14 also controls the activity of the core component in the PI3K complex, beclin-1/Atg6, by maintaining its phosphorylation state.[44,45] Atg14 is transcriptionally regulated by forkhead box O1 (FOXO1) in the liver and is involved in lipid metabolism.[46] Interestingly, FOXO1 is also a direct target of miR-135a activity, adding another level of regulation.[38] Thus, the suppressive role in autophagy by miR-135a could be crucial for tumor development within a specific microenvironment affected by circulating factors such as FVII in the liver sinusoids and might be an earlier molecular event than those which have been described before. We also found that autophagic suppression by miR-135a was responsible for down-regulation of adenosine monophosphate-activated protein kinase alpha2 (AMPKα2) in vitro (data not shown), which might play a pivotal role in inhibition of early transformation and progression events in HCC and therefore needs further investigation.

In conclusion, our current study provides novel evidence that TF/FVII/PAR2 signaling regulates miRNA levels to modulate the autophagic process in HCC. Herein, we describe new findings in which upregulation of miR-135a is highly associated with HCC progression as a result of decreased levels of its direct target, Atg14. Therefore, antagonizing PAR2 signaling and/or miR-135a activity may be a useful strategy to control certain malignant behaviors of HCC. However, although aberrant miR-135a levels have been frequently observed in various types of cancers, the biological outcomes of miR-135a deregulation can largely depend upon cellular context.[47,48] Careful examination is required for potential future diagnostic and therapeutic purposes.

MATERIALS AND METHODS

Clinical Sample Collection

The clinical study was approved by the Internal Review Board of Kaohsiung Chang Gung Memorial Hospital (approval numbers 100-3002A3 and 105-1587C). HCC tissues and corresponding adjacent non-tumorous counterparts were collected from patients who underwent curative hepatic resection from August 2010 to July 2015. The inclusion criteria were as follows: (1) diagnosis with primary HCC, (2) hepatic resection as the first treatment protocol, (3) willing to give written informed consent for sample collection before surgical procedures, and (4) an age above 20 years. None of the patients received prior chemotherapy or loco-regional therapies before surgical resection. The demographics and clinicopathological characteristics were recorded and summarized in Table 2. HCC staging and T-M-N classification were based on *The American Joint Committee on Cancer (AJCC) Cancer Staging Manual, 7th Edition*. The patients were followed at the outpatient clinic with regular surveillance for recurrence by serum α-fetoprotein level and ultrasound every three months and/or contrast-enhanced tomography if recurrent tumor was suspected.

Cell Culture and Treatment

The human HCC cell lines Hep3B and HepG2 were purchased from the Bioresource Collection and Research Center (BCRC, Taiwan). The cells were maintained in low-glucose DMEM supplemented with 10% fetal bovine serum (FBS), 100 µg/mL streptomycin, and 100 U/mL penicillin and incubated at a 37°C, 5% CO_2 atmosphere. Recombinant TF and FVII were purchased from R&D Systems (Minneapolis, MN, USA). PAR2 peptide agonist SLIGKV-NH_2 was purchased from Peptides International (Louisville, KY, USA). The optimal concentrations of reagents were tested in pilot studies and used as indicated in respective experiments.

RNA Isolation and miRNA Sequencing Analysis

Total RNA was purified from the samples using the RNeasy kit from QIAGEN (Valencia, CA, USA) according to the manufacturer's protocol. After elution in 100 µL nuclease-free water, the total RNA was precipitated by mixing eluate with 3 M final concentration of ammonium acetate, adding 4 volumes of ethanol and chilled overnight at −20°C. The pellet was washed with 80% ethanol, centrifuged at 16,000 × *g* for 30 min three times, and then subjected to 15%

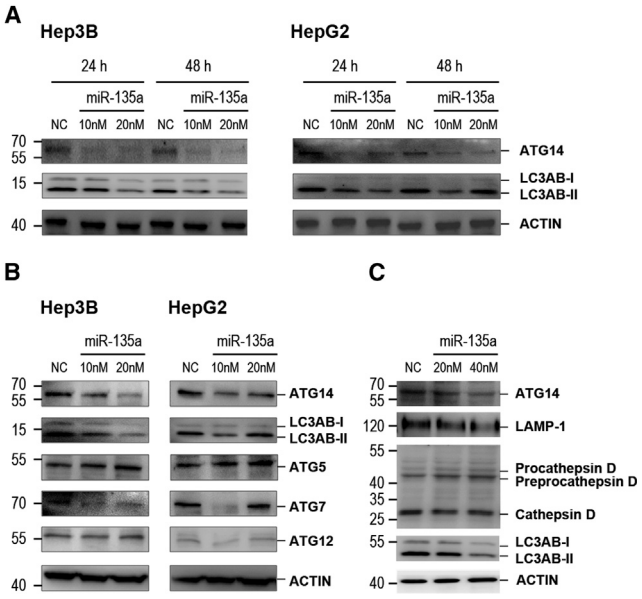

Figure 4. miR-135a Inhibits the Autophagy Pathway In Vitro

(A) Hep3B and HepG2 cells were transfected with a miR-135a mimic (final concentrations, 10 nM, 20 nM), and protein levels of Atg14 and LC3A/B were determined after 24 hr using immunoblotting. (B) Protein levels of Atg5, Atg7, and Atg12 were examined in miR-135a-transfected Hep3B cells. (C) Hep3B cells were transfected with a miR-135a mimic (final concentrations, 20 nM, 40 nM) for 24 hr. Protein levels of LAMP-1, cathepsin D, and LC3A/B were determined. Precursor and mature forms of cathepsin D are indicated. Densitometric values are presented as fold changes over the controls (set as 1) and are shown below each lane of the blot.

denaturing PAGE. The 18- to 30-nt size range of RNA was isolated from the gel and purified. Solexa proprietary adaptors were sequentially ligated to the ends of these small RNAs.

The ligation products were then purified and converted to complementary DNA according to the manufacturer's instructions of TruSeq Small RNA Kit (Illumina, San Diego, USA). Afterward, the purified libraries were sized and quantified, and the quality was controlled by Agilent High Sensitivity DNA Kit on Agilent 2100 Bioanalyzer System (Agilent Technologies, Böblingen, Germany). All small RNA bar-coded pooled libraries were clustered using TruSeq V3 flow cells and sequenced using Illumina Genome Analyzer. Data analysis and base calling were accomplished using the Strand NGS 2.1 software (Strand Life Sciences, Bangalore, Karnataka, India).

qRT-PCR

Total RNA was extracted using the RNeasy Mini Kit (QIAGEN) according to the manufacturer's instructions. For mRNA detection, first-strand cDNA was synthesized with 1 μg total RNA using the High Capacity Reverse Transcriptase (Applied Biosystems; Grand Island, NY, USA). qRT-PCR was performed using the SYBR Green PCR Master Mix with specific TaqMan Assay probes (Thermo Fisher Scientific; Waltham, MA, USA) or pre-designed primers on an ABI 7500 fast PCR system (Applied Biosystems). To quantify miRNA levels, TaqMan MicroRNA Reverse Transcription Kit and TaqMan Fast Universal PCR Master Mix were used with specific TaqMan miRNA probes (Applied Biosystems). Amplifications were carried out with an initial denaturation at 95°C for 20 s, followed by 40 cycles of 95°C for 3 s and 60°C for 30 s. Relative mRNA or miRNA expression was calculated against GAPDH, actin, or U6 rRNA using the ΔΔCt method.

Immunoblotting

Whole-cell extracts were prepared by solubilizing cells in cell lysis buffer containing protease and phosphatase inhibitors (Roche Diagnostics; Basel, Switzerland). Protein concentration was determined using BCA Assay (Thermo Fisher Scientific; Waltham, MA, USA). For western detection, equal quantities of protein were resolved on 10% SDS polyacrylamide gels and transferred onto nitrocellulose membranes. Following blocking in 5% non-fat dried milk in Tris-buffered saline (TBS), the membranes were incubated with primary antibodies prepared in TBS with 0.05% Tween 20 (TBST) at 4°C overnight. After suitable washes with TBST, the membranes were incubated with appropriate secondary antibodies (1:5,000 or 10,000) prepared in TBST. Protein bands were visualized using the enhanced chemiluminescence (ECL) western blot detection reagents (Millipore; Billerica, MA, USA) and scanned using the G:BOX iChemi XL imaging system (J&H Technology; Bradenton, FL, USA). The primary antibodies used in this study are listed as follows: TF (sc-59714, Santa Cruz Biotechnology; Santa Cruz, CA, USA); FVII (Ab97614, Abcam; Cambridge, UK); PAR2 (sc-13504, Santa Cruz Biotechnology); LC3A/B (L8918, Sigma-Aldrich); LAMP-1 (sc-5570, Santa Cruz Biotechnology); Atg5 (sc-133158, Santa Cruz Biotechnology); Atg7 (sc-376212, Santa Cruz Biotechnology); Atg12 (sc-271688, Santa Cruz Biotechnology); and Atg14 (5504, Cell Signaling; Danvers, MA, USA). To ensure equal loading, membranes were stripped and reprobed with anti-β-actin (LV158863, Millipore).

Transfection of siRNAs and miRNAs

Transient transfection of siRNAs against TF (sc-44984, Santa Cruz Biotechnology), FVII (sc-40401), PAR-2 (sc-36188), or miR-135a mimic (Thermo Fisher Scientific) was conducted in Hep3B cells in 6-well plates using GenMute siRNA transfection reagent (SignaGen Laboratories; Rockville, MD, USA) according to manufacturer's recommendations, and a final concentration of 10, 20, or 40 nM of siRNA/miRNA was used accordingly. Cells were harvested for protein or total RNA extraction 24 or 48 hr after transfection as indicated in each experiment.

Dual-Luciferase Reporter Assay

The putative miR-135a target sequence (predicted by miRDB; http://mirdb.org) from the 3′ UTR of Atg14 gene was synthesized (Thermo Fisher Scientific) as individual oligonucleotide pairs so that when these pairs were annealed, overhangs that corresponded to XhoI and XbaI digested sequence would flank the miRNA target region. Annealed oligonucleotides were then ligated into pmirGLO vector (Promega; Madison, WI, USA) digested with the same restriction

enzymes. Sequence analysis was performed on plasmids acquired. Plasmids containing the mutated miR-135a target sequence were also constructed in parallel.

Plasmid DNA was purified from bacterial culture using QIAGEN Plasmid Mini Kit (QIAGEN). For the dual-luciferase reporter assay, the construct that contained the miR-135a target site or mutated sequence was transfected along with miR-135a mimic or control miRNA into Hep3B cells using GenMute transfection reagent. Twenty-four hours after transfection, cells were harvested and analyzed for firefly and Renilla luciferase bioluminescence using the Dual-Glo Luciferase Assay System (Promega) on the Victor X4 multibel reader (PerkinElmer; Waltham, MA, USA). The data were presented as the ratio of firefly to Renilla luciferase activity.

Statistical Analysis

Categorical variables were compared using the chi-square test (or Fisher's exact test where appropriate). Survival rates were determined using the Kaplan-Meier method, and the differences in survival were compared using the log rank test. Pearson's correlation was used for correlation analysis. For in vitro experiments, statistical significance was determined using ANOVA against the control group. All tests were performed using the SPSS 15.0 software (SPSS; Chicago, IL, USA). A p value < 0.05 was considered statistically significant.

AUTHOR CONTRIBUTIONS

Conceptualization, K.-D.C., C.-C.L., K.-T.H.; Methodology, K.-D.C., K.-T.H., L.-W.H., Y.-W.C.; Investigation, I.-Y.K., M.-C.T., C.-H.W., L.-Y.C., C.-P.K.; Writing – Original Draft, K.-T.H., K.-D.C.; Writing – Review and Editing, K.-T.H., C.-C.L., K.-D.C.; Funding Acquisition, K.-D.C., C.-C.L,. C.-L.C.; Resource, Y.-F.C., S.G., C.-C.L.; Supervision, Y.-F.C., C.-L.C.

CONFLICTS OF INTEREST

The authors declare no conflicts of interest.

ACKNOWLEDGMENTS

This work was supported by grants from the following sources: Ministry of Science and Technology of Taiwan (MOST 104-2314-B-182A-018 and MOST 105-2314-B-182A-037-MY2 to C.-L.C. and MOST 104-2314-B-182A-089-MY3 to Y.-F.C.) and Chang Gung Memorial Hospital (CMRPG8C1151, CMRPG8D1032, and CMRPG8D1033 to K.-T.H.; CMRPG8D0561, CMRPG8D0751, CMRPG8D1022, and CMRPG8D1023 to K.-D.C.; CMRPG8A1203 and CMRPG8E1651 to C.-C.L.; and CMRPG8C0952 and CMRPG8D1012 to C.-L.C.). We also thank the Tissue Bank Core Lab at Kaohsiung Chang Gung Memorial Hospital (CLRPG8B0033, CLRPG8E0161, and CMRPG8D0062 to Y.-W.C.) for excellent technical support.

REFERENCES

1. Siegel, R., Ma, J., Zou, Z., and Jemal, A. (2014). Cancer statistics, 2014. CA Cancer J. Clin. *64*, 9–29.
2. Singal, A.G., and El-Serag, H.B. (2015). Hepatocellular carcinoma from epidemiology to prevention: translating knowledge into practice. Clin. Gastroenterol. Hepatol. *13*, 2140–2151.
3. Jemal, A., Bray, F., Center, M.M., Ferlay, J., Ward, E., and Forman, D. (2011). Global cancer statistics. CA Cancer J. Clin. *61*, 69–90.
4. Bruix, J., and Sherman, M.; American Association for the Study of Liver Diseases (2011). Management of hepatocellular carcinoma: an update. Hepatology *53*, 1020–1022.
5. Graf, D., Vallböhmer, D., Knoefel, W.T., Kröpil, P., Antoch, G., Sagir, A., and Häussinger, D. (2014). Multimodal treatment of hepatocellular carcinoma. Eur. J. Intern. Med. *25*, 430–437.
6. Carthew, R.W., and Sontheimer, E.J. (2009). Origins and mechanisms of miRNAs and siRNAs. Cell *136*, 642–655.
7. He, L., and Hannon, G.J. (2004). MicroRNAs: small RNAs with a big role in gene regulation. Nat. Rev. Genet. *5*, 522–531.
8. Macfarlane, L.A., and Murphy, P.R. (2010). MicroRNA: biogenesis, function and role in cancer. Curr. Genomics *11*, 537–561.
9. Chen, X., Ba, Y., Ma, L., Cai, X., Yin, Y., Wang, K., Guo, J., Zhang, Y., Chen, J., Guo, X., et al. (2008). Characterization of microRNAs in serum: a novel class of biomarkers for diagnosis of cancer and other diseases. Cell Res. *18*, 997–1006.
10. Mitchell, P.S., Parkin, R.K., Kroh, E.M., Fritz, B.R., Wyman, S.K., Pogosova-Agadjanyan, E.L., Peterson, A., Noteboom, J., O'Briant, K.C., Allen, A., et al. (2008). Circulating microRNAs as stable blood-based markers for cancer detection. Proc. Natl. Acad. Sci. USA *105*, 10513–10518.
11. Hou, J., Lin, L., Zhou, W., Wang, Z., Ding, G., Dong, Q., Qin, L., Wu, X., Zheng, Y., Yang, Y., et al. (2011). Identification of miRNomes in human liver and hepatocellular carcinoma reveals miR-199a/b-3p as therapeutic target for hepatocellular carcinoma. Cancer Cell *19*, 232–243.
12. Qi, P., Cheng, S.Q., Wang, H., Li, N., Chen, Y.F., and Gao, C.F. (2011). Serum microRNAs as biomarkers for hepatocellular carcinoma in Chinese patients with chronic hepatitis B virus infection. PLoS ONE *6*, e28486.
13. Chuang, K.H., Whitney-Miller, C.L., Chu, C.Y., Zhou, Z., Dokus, M.K., Schmit, S., and Barry, C.T. (2015). MicroRNA-494 is a master epigenetic regulator of multiple invasion-suppressor microRNAs by targeting ten eleven translocation 1 in invasive human hepatocellular carcinoma tumors. Hepatology *62*, 466–480.
14. Zhou, J.N., Zeng, Q., Wang, H.Y., Zhang, B., Li, S.T., Nan, X., Cao, N., Fu, C.J., Yan, X.L., Jia, Y.L., et al. (2015). MicroRNA-125b attenuates epithelial-mesenchymal transitions and targets stem-like liver cancer cells through small mothers against decapentaplegic 2 and 4. Hepatology *62*, 801–815.
15. Lin, L., and Baehrecke, E.H. (2015). Autophagy, cell death, and cancer. Mol. Cell. Oncol. *2*, e985913.
16. Galluzzi, L., Pietrocola, F., Bravo-San Pedro, J.M., Amaravadi, R.K., Baehrecke, E.H., Cecconi, F., Codogno, P., Debnath, J., Gewirtz, D.A., Karantza, V., et al. (2015). Autophagy in malignant transformation and cancer progression. EMBO J. *34*, 856–880.
17. Kondo, Y., Kanzawa, T., Sawaya, R., and Kondo, S. (2005). The role of autophagy in cancer development and response to therapy. Nat. Rev. Cancer *5*, 726–734.
18. Yang, Z.J., Chee, C.E., Huang, S., and Sinicrope, F.A. (2011). The role of autophagy in cancer: therapeutic implications. Mol. Cancer Ther. *10*, 1533–1541.
19. Ding, Z.B., Shi, Y.H., Zhou, J., Qiu, S.J., Xu, Y., Dai, Z., Shi, G.M., Wang, X.Y., Ke, A.W., Wu, B., and Fan, J. (2008). Association of autophagy defect with a malignant phenotype and poor prognosis of hepatocellular carcinoma. Cancer Res. *68*, 9167–9175.
20. Rautou, P.E., Mansouri, A., Lebrec, D., Durand, F., Valla, D., and Moreau, R. (2010). Autophagy in liver diseases. J. Hepatol. *53*, 1123–1134.
21. Chen, K.D., Huang, K.T., Tsai, M.C., Wu, C.H., Kuo, I.Y., Chen, L.Y., Hu, T.H., Chen, C.L., and Lin, C.C. (2016). Coagulation factor VII and malignant progression of hepatocellular carcinoma. Cell Death Dis. *7*, e2110.
22. Chen, K.D., Wang, C.C., Tsai, M.C., Wu, C.H., Yang, H.J., Chen, L.Y., Nakano, T., Goto, S., Huang, K.T., Hu, T.H., et al. (2014). Interconnections between autophagy and the coagulation cascade in hepatocellular carcinoma. Cell Death Dis. *5*, e1244.

23. Tsai, M.C., Chen, K.D., Wang, C.C., Huang, K.T., Wu, C.H., Kuo, I.Y., Chen, L.Y., Hu, T.H., Goto, S., Nakano, T., et al. (2015). Factor VII promotes hepatocellular carcinoma progression through ERK-TSC signaling. Cell Death Dis. *1*, 15051.

24. Lin, C.C., and Chen, C.L. (2016). Living donor liver transplantation for hepatocellular carcinoma achieves better outcomes. Hepatobiliary Surg. Nutr. *5*, 415–421.

25. Bronte, F., Bronte, G., Fanale, D., Caruso, S., Bronte, E., Bavetta, M.G., Fiorentino, E., Rolfo, C., Bazan, V., Di Marco, V., and Russo, A. (2016). HepatomiRNoma: the proposal of a new network of targets for diagnosis, prognosis and therapy in hepatocellular carcinoma. Crit. Rev. Oncol. Hematol. *97*, 312–321.

26. Hayes, C.N., and Chayama, K. (2016). MicroRNAs as biomarkers for liver disease and hepatocellular carcinoma. Int. J. Mol. Sci. *17*, 280.

27. Mizuguchi, Y., Takizawa, T., Yoshida, H., and Uchida, E. (2016). Dysregulated miRNA in progression of hepatocellular carcinoma: a systematic review. Hepatol. Res. *46*, 391–406.

28. Darmoul, D., Gratio, V., Devaud, H., and Laburthe, M. (2004). Protease-activated receptor 2 in colon cancer: trypsin-induced MAPK phosphorylation and cell proliferation are mediated by epidermal growth factor receptor transactivation. J. Biol. Chem. *279*, 20927–20934.

29. Kaufmann, R., Oettel, C., Horn, A., Halbhuber, K.J., Eitner, A., Krieg, R., Katenkamp, K., Henklein, P., Westermann, M., Böhmer, F.D., et al. (2009). Met receptor tyrosine kinase transactivation is involved in proteinase-activated receptor-2-mediated hepatocellular carcinoma cell invasion. Carcinogenesis *30*, 1487–1496.

30. Su, S., Li, Y., Luo, Y., Sheng, Y., Su, Y., Padia, R.N., Pan, Z.K., Dong, Z., and Huang, S. (2009). Proteinase-activated receptor 2 expression in breast cancer and its role in breast cancer cell migration. Oncogene *28*, 3047–3057.

31. Gieseler, F., Ungefroren, H., Settmacher, U., Hollenberg, M.D., and Kaufmann, R. (2013). Proteinase-activated receptors (PARs) - focus on receptor-receptor-interactions and their physiological and pathophysiological impact. Cell Commun. Signal. *11*, 86.

32. Albrektsen, T., Sørensen, B.B., Hjortø, G.M., Fleckner, J., Rao, L.V., and Petersen, L.C. (2007). Transcriptional program induced by factor VIIa-tissue factor, PAR1 and PAR2 in MDA-MB-231 cells. J. Thromb. Haemost. *5*, 1588–1597.

33. Liu, Y., and Mueller, B.M. (2006). Protease-activated receptor-2 regulates vascular endothelial growth factor expression in MDA-MB-231 cells via MAPK pathways. Biochem. Biophys. Res. Commun. *344*, 1263–1270.

34. Wu, B., Zhou, H., Hu, L., Mu, Y., and Wu, Y. (2013). Involvement of PKCα activation in TF/VIIa/PAR2-induced proliferation, migration, and survival of colon cancer cell SW620. Tumour Biol. *34*, 837–846.

35. Chen, Y., Zhang, J., Wang, H., Zhao, J., Xu, C., Du, Y., Luo, X., Zheng, F., Liu, R., Zhang, H., and Ma, D. (2012). miRNA-135a promotes breast cancer cell migration and invasion by targeting HOXA10. BMC Cancer *12*, 111.

36. Leung, C.O., Deng, W., Ye, T.M., Ngan, H.Y., Tsao, S.W., Cheung, A.N., Pang, R.T., and Yeung, W.S. (2014). miR-135a leads to cervical cancer cell transformation through regulation of β-catenin via a SIAH1-dependent ubiquitin proteosomal pathway. Carcinogenesis *35*, 1931–1940.

37. Nagel, R., le Sage, C., Diosdado, B., van der Waal, M., Oude Vrielink, J.A., Bolijn, A., Meijer, G.A., and Agami, R. (2008). Regulation of the adenomatous polyposis coli gene by the miR-135 family in colorectal cancer. Cancer Res. *68*, 5795–5802.

38. Ren, J.W., Li, Z.J., and Tu, C. (2015). MiR-135 post-transcriptionally regulates FOXO1 expression and promotes cell proliferation in human malignant melanoma cells. Int. J. Clin. Exp. Pathol. *8*, 6356–6366.

39. Matsuzawa, S.I., and Reed, J.C. (2001). Siah-1, SIP, and Ebi collaborate in a novel pathway for beta-catenin degradation linked to p53 responses. Mol. Cell *7*, 915–926.

40. Petracco, R., Grechukhina, O., Popkhadze, S., Massasa, E., Zhou, Y., and Taylor, H.S. (2011). MicroRNA 135 regulates HOXA10 expression in endometriosis. J. Clin. Endocrinol. Metab. *96*, E1925–E1933.

41. Liu, S., Guo, W., Shi, J., Li, N., Yu, X., Xue, J., Fu, X., Chu, K., Lu, C., Zhao, J., et al. (2012). MicroRNA-135a contributes to the development of portal vein tumor thrombus by promoting metastasis in hepatocellular carcinoma. J. Hepatol. *56*, 389–396.

42. Obara, K., Sekito, T., Niimi, K., and Ohsumi, Y. (2008). The Atg18-Atg2 complex is recruited to autophagic membranes via phosphatidylinositol 3-phosphate and exerts an essential function. J. Biol. Chem. *283*, 23972–23980.

43. Matsunaga, K., Morita, E., Saitoh, T., Akira, S., Ktistakis, N.T., Izumi, T., Noda, T., and Yoshimori, T. (2010). Autophagy requires endoplasmic reticulum targeting of the PI3-kinase complex via Atg14L. J. Cell Biol. *190*, 511–521.

44. Fogel, A.I., Dlouhy, B.J., Wang, C., Ryu, S.W., Neutzner, A., Hasson, S.A., Sideris, D.P., Abeliovich, H., and Youle, R.J. (2013). Role of membrane association and Atg14-dependent phosphorylation in beclin-1-mediated autophagy. Mol. Cell. Biol. *33*, 3675–3688.

45. Kim, J., Kim, Y.C., Fang, C., Russell, R.C., Kim, J.H., Fan, W., Liu, R., Zhong, Q., and Guan, K.L. (2013). Differential regulation of distinct Vps34 complexes by AMPK in nutrient stress and autophagy. Cell *152*, 290–303.

46. Xiong, X., Tao, R., DePinho, R.A., and Dong, X.C. (2012). The autophagy-related gene 14 (Atg14) is regulated by forkhead box O transcription factors and circadian rhythms and plays a critical role in hepatic autophagy and lipid metabolism. J. Biol. Chem. *287*, 39107–39114.

47. Wan, X., Pu, H., Huang, W., Yang, S., Zhang, Y., Kong, Z., Yang, Z., Zhao, P., Li, A., Li, T., and Li, Y. (2016). Androgen-induced miR-135a acts as a tumor suppressor through downregulating RBAK and MMP11, and mediates resistance to androgen deprivation therapy. Oncotarget *7*, 51284–51300.

48. Zhou, H., Guo, W., Zhao, Y., Wang, Y., Zha, R., Ding, J., Liang, L., Yang, G., Chen, Z., Ma, B., and Yin, B. (2014). MicroRNA-135a acts as a putative tumor suppressor by directly targeting very low density lipoprotein receptor in human gallbladder cancer. Cancer Sci. *105*, 956–965.